INSTITUTE OF PHYSICS PUBLISHING JOURNAL OF PHYSICS A: MATHEMATICAL AND GENERAL

J. Phys. A: Math. Gen. **38** (2005) 6689–6702 doi:10.1088/0305-4470/38/30/005

Competing associations in six-species predator–prey models

György Szabó

Research Institute for Technical Physics and Materials Science, PO Box 49, H-1525 Budapest, Hungary

Received 11 February 2005, in final form 13 June 2005
Published 13 July 2005
Online at stacks.iop.org/JPhysA/38/6689

Abstract

We study a set of six-species ecological models where each species has two predators and two prey. On a square lattice the time evolution is governed by iterated invasions between the neighbouring predator–prey pairs chosen at random and by a site exchange with a probability X_s between the neutral pairs. These models involve the possibility of spontaneous formation of different defensive alliances whose members protect each other from the external invaders. The Monte Carlo simulations show a surprisingly rich variety of the stable spatial distributions of species and subsequent phase transitions when tuning the control parameter X_s. These very simple models are able to demonstrate that the competition between these associations influences their composition. Sometimes the dominant association is developed via a domain growth. In other cases larger and larger invasion processes precede the prevalence of one of the stable associations. Under some conditions the survival of all the species can be maintained by the cyclic dominance occurring between these associations.

PACS numbers: 87.23.Cc, 05.50.+q, 64.60.Cn

1. Introduction

Ecological systems exhibit a large number of associations of certain species which coexist on the same territory. These associations can be considered as evolutionary stable states (or Nash equilibria) whose stability and competitiveness depend on the environmental conditions [1–6]. Generally, the systematic analysis of the competition between these spatial states is made difficult by the complexity of the phenomena and by the large number of parameters in the suitable models.

In order to have a deeper insight into these phenomena, we consider now a family of toy models exemplifying some basic features and the richness of possible behaviour. In these predator–prey models the species, located on the sites of a lattice, invades one of the

neighbouring sites if it is occupied by its prey. The investigation of predator–prey systems on lattices has a long history reviewed recently in the papers [5, 7, 8]. In these systems the invasion processes can yield extinction of species and/or maintain some steady states in the spatial distribution if the corresponding food web (a directed graph) contains loops. In such a situation a self-organizing spatio-temporal pattern can be formed by the species dominating each other cyclically. Besides this, in the present model the neutral (neighbouring) species are allowed to exchange their sites. This latter process helps the formation of many well-mixed distributions of neutral species which can also protect each other against the rest of the species. As a result these models possess many final states towards which such a system can evolve. In the spatial systems these states can coexist by forming domains if the system is started from a random initial state for sufficiently large sizes. The competition between these multi-species associations along the boundaries can affect their internal structure and the evolutionary process selects one of these states. Thus, the investigation of these simplified models can help us to clarify some mechanisms related to Darwinian selection [1] and the emergence of structural complexity [9] characterizing *pre-biotic* evolution too [10].

Several basic features are already well known for the simplest versions of the above models. As mentioned above, if the spatial predator–prey model on the square lattice contains three species with cyclic dominance (this model is also called the spatial rock–scissors–paper game), then the cyclic invasions maintain a self-organizing pattern with equal species concentrations [11–13]. Both the composition [14, 15] and the geometrical features [16, 17] of this spatial pattern are affected by the independent variation of invasion rates, meanwhile this structure provides stability against some external invaders [18, 19]. A similar self-organizing pattern is found for those cyclic predator–prey (or voter) models where the number N_s of species is limited, namely $3 < N_s \leqslant 14$ [13]. For even N_s, however, these systems are very sensitive to the independent variation of invasion rates [20]. More complex behaviour was observed for those systems where the food web consists of several cycles that can be distinguished from a topological point of view [19]. In these multi-cycle ecological models the final (stationary) state is prevalently a defensive alliance, being the most stable cyclic subsystem. These defensive alliances are composed of those species that form a cycle in the food web, thereby their spatial distribution is equivalent to those of one-cycle systems mentioned above. The privileged role of these associations is related to their most effective protection, provided by the topological features of the food web, against the external species. In their enhanced protection the role of spatial structure is crucial because under mean-field conditions these associations are not able to eliminate the external invaders.

Very recently the investigation of a four-species cyclic predator–prey model has indicated the spontaneous formation of another type of defensive alliance [21]. In this latter model the lattice sites can be empty and the individuals are allowed to jump to one of the neighbouring empty sites. As a result the odd (even) label species can form a well-mixed state ensuring the possibility of prompt counter-attack against the even (odd) label species and by this means these associations can defend their territories. In other words, the neutral species can also form defensive alliances in the presence of some local mixing.

In this paper we consider a set of models allowing the appearance of both types of above-mentioned defensive alliances. In these six-species models the food web contains many cycles and the local mixing is provided by a site exchange between the neutral pairs. For all the models the probability X_s of site exchange will be the only tunable parameter. Using Monte Carlo (MC) simulations it will be shown that, despite their simplicity, these models are able to account for different stationary states and subsequent phase transitions when varying the value of X_s. The stationary states are composed of different species whose number varies from 2 to 6. Evidently, the time scales of the formation of these states are dependent on the microscopic

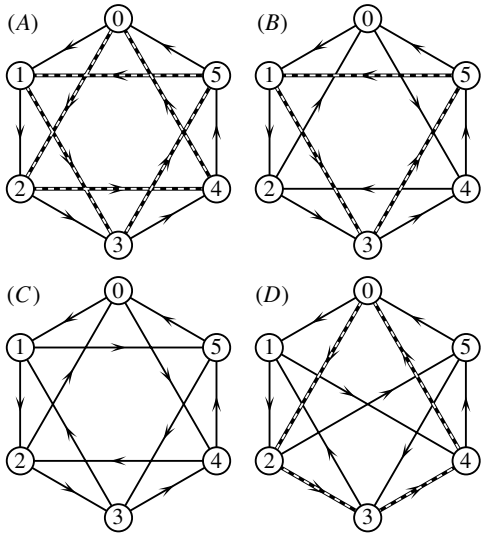

Figure 1. Food webs defining the four classes of predator–prey relations where each species has two predators and two prey. The decorated lines connect the members of the defensive alliances providing mutual protection against the external invaders via cyclic invasions.

mechanism (invasion or mixing). Sometimes equivalent states are formed via a nucleation mechanism and they can destroy each other (cyclically) when the boundaries of these growing domains meet.

Apparently the combination of our previous models [19, 21] means a simple extension of the six-species models. This extension, however, exemplifies that a small variation of a sufficiently complex ecological model can yield a surprisingly large increase in the types of behaviour and phase transitions whose clarification raises many other questions. At the same time, many aspects of these features seem to be valid for sufficiently complex ecological systems (or evolutionary games) as discussed in the conclusions.

2. Spatial predator–prey models

In all the present models the site i of a square lattice is occupied by an individual belonging to one of the six species and the corresponding distribution is given by a set of site variables ($s_i = 0, \ldots, 5$). The predator–prey relation between the species is defined by a food web. On the corresponding directed graph the nodes (labelled from 0 to 5) refer to the species and the directed edges point to the prey from its predator. Our analysis is focused on those systems where each species has two predators, two prey and a neutral one (not linked). In this case each possible food web (satisfying the above conditions) is isomorphic to one of the four graphs shown in figure 1 and the corresponding model is named after their labels A, B, C and D [19].

The evolution of the species distribution is governed by iterating nearest neighbour invasions and site exchanges. More precisely, starting from a random initial state we repeat the following steps: (1) two nearest-neighbour sites are chosen at random; (2) if these sites are occupied by a predator–prey pair, then the prey is killed and an offspring of the predator occupies the site of the prey; (3) for neutral pairs the species exchange their sites with a

probability X_s. Evidently, nothing happens if the individuals belong to the same species. For example, in the model A the randomly chosen pair (1, 2) transforms into (1, 1) (invasion) and the pair (1, 4) transform to (4, 1) (site exchange) with a probability X_s, otherwise the neutral pair remains unchanged. Note that the invasion rates between the predator–prey pairs are unique, and the models have only one parameter (X_s) characterizing the strength of mixing between the neutral species.

These models are investigated by a series of MC simulations performed on a square lattice with sites $N = L \times L$ under periodic boundary conditions at different values of X_s. The simulations are started from a random initial state. Within a time unit (MCS) each pair has a chance once on average to perform an invasion (between predator and prey) or a site exchange with a probability X_s (between neutral species). During the simulations we have recorded the current values of species concentrations ($\rho_\alpha(t)$; $\alpha = 0, \ldots, 5$) as well as the probability of finding predator–prey ($P_{\rm pp}(t)$) and neutral pairs $P_n(t)$ on two neighbouring sites. The stationary states are characterized by the average values of these quantities (denoted as ρ_α, $P_{\rm pp}$ and P_n) which are determined by averaging over a long sampling time varied from 10^4 to 10^6 MCS after a suitable thermalization time. Evidently, $\sum_\alpha \rho_\alpha = 1$ and the quantity $1 - P_{\rm pp} - P_n$ gives the probability of finding the same species on two neighbouring sites. At the same time we have determined the fluctuation of these quantities defined as $\chi_\alpha = N\left[\langle\rho_\alpha^2\rangle - \langle\rho_\alpha\rangle^2\right]$, where $\langle\cdots\rangle$ refers to the averaging over the sampling time. To avoid undesired size effects, the linear size is varied from $L = 500$ to 2500. The larger sizes are used in the close vicinity of transition points where the fluctuations diverge.

Now we discuss the general features of the possible stationary states. For all these models there exist six homogeneous states denoted as $\Phi_\alpha^{(h)}$ where $s_i = \alpha$ ($\alpha = 0, \ldots, 5$) for each site i. These states remain unchanged and the evolution of the species distribution is stopped whenever one of these (absorbing) states is reached. At the same time, the homogeneous state is unstable against the invasion of suitable predators.

The mixed states of neutral species are denoted as $\Phi_{03}^{(n)}$ if $s_i = 0$ or 3. Evidently, there exist two additional neutral pairs for all four models. In such a state there are no invasions at all. Consequently, the ratio of populations is fixed during the evolution meanwhile the system tends towards an uncorrelated spatial distribution for $X_s > 0$.

For all four models there exist several three-species associations whose members invade each other cyclically. For example, in model A one of the corresponding states is denoted as $\Phi_{024}^{(c)}$ where the subscripts refer to the three species being present with the same average concentrations, $\rho_0 = \rho_2 = \rho_4 = 1/3$. The corresponding spatial distribution is maintained by the cyclic invasions yielding a short average lifetime for the individuals (the survival probability of individuals decreases exponentially with relaxation time $\tau \simeq 1.8$ MCS) and the correlation length ($\xi \simeq 2.5$) characterizes the typical domain size [11, 13, 22]. In general, the stability of the possible three-species associations against the external invaders is determined by the food web topology [19]. For the model A the food web contains only two equivalent three-species cycles which are called defensive alliances because their members protect each other cyclically against the external invaders. For example, within the state $\Phi_{024}^{(c)}$ the species 2 can only be invaded by the 'external' species 1. During the cyclic invasion processes, both the internal species 2 and the substituted invader 1 are killed by their common predator (0); in the meantime the third member (4) of the association feeds the species 2 and blocks the spreading of invaders. Thus, sooner or later the offspring of invaders will be eliminated from the system. One can easily check that other types (3 or 5) of invaders become extinct in the same way because of the cyclic symmetry in this food web. For the food web B the system has only one cyclic defensive alliance $\left(\Phi_{135}^{(c)}\right)$ that will dominate the final stationary state although this food web has four additional three-species cycles with

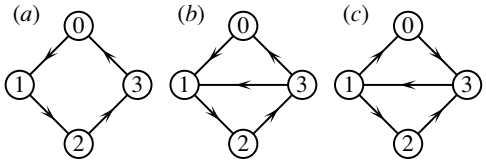

Figure 2. Food webs for the four-species subsystems.

lower stability. Model C has eight equivalent three-species cycles, and neither of them can be considered as a defensive alliance in the sense mentioned above.

Model D represents another situation where one can find four three-species and three four-species cycles. In this case the four-species cycle $\Phi^{(c)}_{0234}$ proved to be the most stable spatial association that satisfies the conditions to be a cyclic defensive alliance [19].

For $X_s = 0$, the stability of the different states was already determined in a previous study when considering the effect of mutations on the population in similar six-species predator–prey models [19]. The present analysis will be focused on the effect of site exchange between the neutral pairs ($X_s > 0$) in the absence of mutation. For small sizes all the above-mentioned states can be observed as a final state. For sufficiently large system sizes, however, the system tends towards the real stationary state independent of the initial state.

3. Four-species subsystems

In this section we study the behaviour of several four-species subsystems whose understanding will help the interpretation of results obtained for the more complicated systems. More precisely, our analysis is focused on three systems (labelled a, b and c) whose food webs given in figure 2.

The food web of subsystem a is equivalent to a four-species cyclic predator–prey model where each species has only one predator and one prey. Such a situation can occur in the models A, B and D if two species are missing, and its analysis becomes particularly important for model D where $\Phi^{(c)}_{0234}$ is the stable state for $X_s = 0$. In addition, similar cyclic dominance has been reported very recently by Traulsen *et al* [23, 24] considering a four-strategy prisoner's dilemma game.

Some features of this system have already been investigated previously by several authors for $X_s = 0$ [13, 20, 21]. In this case the cyclic invasions maintain a self-organizing pattern with $\rho_0 = \rho_1 = \rho_2 = \rho_3 = 1/4$ and with a probability $P_n = 0.0518(5)$ to find neutral pairs on two neighbouring sites. Here P_n characterize the concentration of interfaces separating neutral domains (e.g., $\Phi^{(h)}_0$ and $\Phi^{(h)}_2$). Along these interfaces the evolution is blocked until one of the invading predators reaches the interface. For $X_s > 0$, however, along these neutral interfaces the site exchange increases the value of P_n and supports the formation of the well-mixed phase of neutral species.

The MC simulations indicate clearly how the value of P_n increases monotonically with X_s upto a threshold value $\left(X_s < X^{(4a)}_{\rm cr} = 0.026\,62(2)\right)$. At the same time the probability $P_{\rm pp}$ of predator–prey pairs is decreasing as shown in figure 3.

Above this threshold value $\left(X_s > X^{(4a)}_{\rm cr}\right)$ the system segregates into two types ($\Phi^{(n)}_{02}$ and $\Phi^{(n)}_{13}$) of growing domains which are mixtures of neutral pairs. During the domain growing processes, these phases are in contact throughout a wide boundary layer (of type $\Phi^{(c)}_{0123}$) which serves as a species reservoir and sets the compositions to be symmetric [21]. Finally, one of

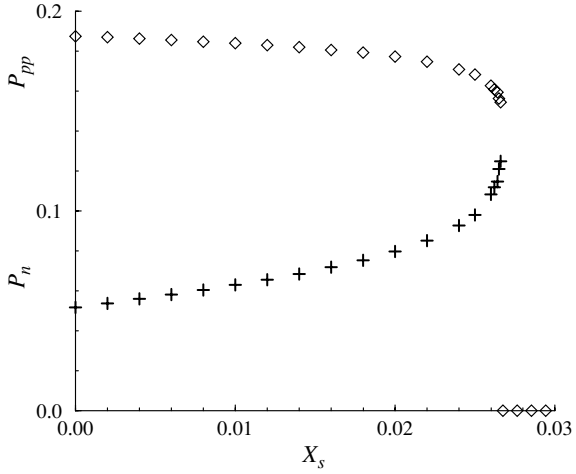

Figure 3. Probability of neutral (pluses) and predator–prey (open diamonds) pairs as a function of X_s for the four-species cyclic food web (see *a* in figure 2).

the two equivalent mixed states will prevail in the whole finite system and then $P_{\rm pp} = 0$ and $P_n = 0.5$.

Subsystem *b* represents the situation when the three-species cyclic defensive alliance $\left(\Phi^{(c)}_{123}\right)$ is attacked by an external invader (of type 0). The MC simulations indicate clearly that after some relaxation process the species 0 dies out and the system remains in the state $\Phi^{(c)}_{123}$ if $X_s < X^{(4b)}_{\rm cr} = 0.0527(1)$. Conversely, the system develops into the symmetric mixed phase $\Phi^{(n)}_{02}$ ($\rho_0 = \rho_2 = 0.5$) for $X_s > X^{(4b)}_{\rm cr}$. In the vicinity of the transition point, the visualization of the species distribution illustrates the formation of domains of $\Phi^{(n)}_{02}$ whose area increases (decreases) slowly above (below) the threshold value. The average velocity of the interfaces (separating the domains of $\Phi^{(n)}_{02}$ and $\Phi^{(c)}_{123}$) seems to be proportional to $X_s - X^{(4b)}_{\rm cr}$ as it is observed for another model [21]. This feature can explain why the ordering process becomes so slow in the close vicinity of the transition point.

The four-species subsystem *c* possesses two equivalent, three-species cycles that have two common species (1 and 3). In this case the spatial distribution of species segregates into two types ($\Phi^{(c)}_{123}$ and $\Phi^{(c)}_{103}$) of growing domains and finally the whole system is dominated by one of them with equal probabilities. Note that the bulk of these phases is not influenced by the site exchange mechanism whose effect is limited to the boundaries separating the phases $\Phi^{(c)}_{123}$ and $\Phi^{(c)}_{103}$. Furthermore, the species within the mixed two-species phase $\Phi^{(n)}_{02}$ are not able to protect each other because species 1 can invade their territories without restraint. This is the reason why the domain growing process is not prevented for $X_s > 0$ and the site exchange causes only a slight variation in the velocity of the growing process.

4. Model *A*

As mentioned above the six-species model *A* has two equivalent three-species cycles consisting of disjoint sets of species, namely $\Phi^{(c)}_{024}$ and $\Phi^{(c)}_{135}$. According to the simulations one of these phases (with equal probability) will overwhelm the whole finite system after a domain growing process if the site exchange probability does not exceed a threshold value, i.e., $X_s < X^{(6A)}_{\rm cr} = 0.055\,92(1)$. On a sufficiently large scale this domain growing process

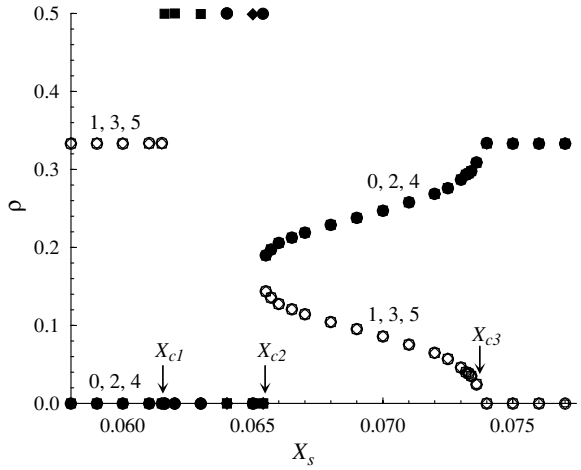

Figure 4. Concentration of species versus X_s. The MC data are denoted by closed circles, open diamonds, closed squares, open circles, closed diamonds and open squares for the species labelled from 0 to 5. The arrows indicate the three transition points.

is similar to those that one can observe for the kinetic Ising model below the critical temperature if the system is started from a random initial state (for a survey of domain growth, see [25]).

Above the threshold value $\left(X_s > X_{\rm cr}^{(6A)}\right)$ the system develops into one of the three (equivalent) two-species states composed from neutral species. The topological features of the food web A imply that the phases $\Phi_{03}^{(n)}$, $\Phi_{14}^{(n)}$ and $\Phi_{25}^{(n)}$ can also be considered as defensive alliances because their members protect each other against the external predators in the well-mixed state. During the transient time one can observe a domain growth with these three types of domains. Apparently this growth is similar to that observed in the three-state Potts model below the critical temperatures [26, 27]. However, along the interfaces separating two domains (say $\Phi_{03}^{(n)}$ and $\Phi_{14}^{(n)}$) there occurs a four-species cycle $\Phi_{0134}^{(c)}$ whose transversal extension is limited by invasions from both sides. Note that the corresponding four-species subsystem (see the food web a in figure 2) exhibits a transition from the four-species cycle ($\Phi_{0134}^{(c)}$ in the mentioned example) to one of the mentioned neutral pair states at $X_s = X_{\rm cr}^{(4a)}$. As $X_{\rm cr}^{(6A)} > X_{\rm cr}^{(4a)}$ therefore the coexistence of the four species is limited to the narrow strips separating the well-mixed phases of the neutral pairs.

The three-colour maps have special points (called three-edge vertices) where three domains meet. Instead of this, here there are patches with phases of either $\Phi_{024}^{(c)}$ or $\Phi_{135}^{(c)}$. This inevitable coexistence of many different phases (during the decomposition processes) may be the reason why $X_{\rm cr}^{(6A)} > X_{\rm cr}^{(4a)}$.

5. Model *B*

In this model very interesting behaviour is found by the MC simulations. One can observe four different phases and three subsequent phase transitions when X_s is increased. It is more surprising that the transition points are very close to each other. To demonstrate the main features, figure 4 illustrates the average values of species concentrations in the stationary states reached by the system starting from a random initial state for different values of X_s. Here the open (closed) symbols are used for the species with odd (even) labels to reduce the confusion

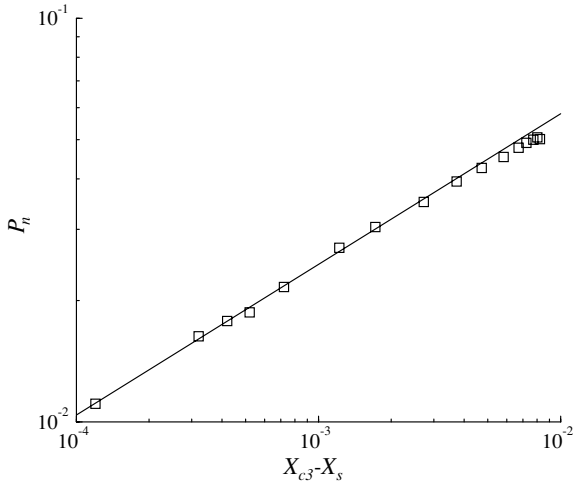

Figure 5. Log–log plot of the MC data (open squares) for the probability of neutral pairs versus $X_{c3}^{(6B)} - X_s$. The fitted power law is denoted by the straight line with a slope of 0.373.

coming from the coincidence of several data. Furthermore, the neutral pairs are denoted by the same type of symbols.

The cyclic defensive alliance $\Phi_{135}^{(c)}$ is proved to be the most stable solution if $X_s < X_{c1}^{(6B)} = 0.061\,55(5)$. In the next region $\left(X_{c1}^{(6B)} < X_s < X_{c2}^{(6B)} = 0.065\,45(5)\right)$ the final stationary state will be equivalent to one of the three well-mixed states of neutral pairs ($\Phi_{03}^{(n)}$, $\Phi_{14}^{(n)}$ and $\Phi_{25}^{(n)}$). All six species survive in the third region of X_s in such a way that $\rho_0 = \rho_2 = \rho_4$ and $\rho_1 = \rho_3 = \rho_5$. If $X_s > X_{c3}^{(6B)} = 0.073\,72(2)$ then only the species with even labels are present and their coexistence with the same concentration is maintained by the cyclic invasions (state $\Phi_{024}^{(c)}$).

The transitions at X_{c1} and X_{c2} can be considered as first order, meanwhile the third one exhibits the features of a continuous (critical) transition. The concentration of the species 1, 3 and 5 vanishes continuously when approaching X_{c3} from below. More precisely, our data are consistent with a power law decrease in the close vicinity of the transition point, that is $\rho_1 = \rho_3 = \rho_5 \simeq (X_{c3} - X_s)^{\beta}$ with $\beta = 0.37(4)$. Similar power law behaviour (with the same exponent) is found for P_n as shown in figure 5. At the same time the MC data show diverging fluctuations for these quantities, which is another relevant feature of the critical transitions. Unfortunately, we could not deduce an adequate (γ) exponent to describe this divergence because of the large statistical uncertainties in these quantities.

In the presence of absorbing state(s), the extinction of a single species in the spatial models has very robust features and the corresponding transition belongs to the directed percolation (DP) universality class characterized by a higher exponent ($\beta_{\mathrm{DP}} = 0.58(2)$ for the two-dimensional systems) [28–31]. In the present model, however, three species die out simultaneously and the background can mediate some interactions among the vanishing species. Evidently, further analysis is necessary to quantify the features of this transition as well as to clarify the reasons causing the distinct behaviour.

In contrary to model A, here the formation of one of the three equivalent well-mixed phases of neutral species is limited to a narrow region $\left(X_{c1}^{(6B)} < X_s < X_{c2}^{(6B)} = 0.065\,45(5)\right)$. The formation of these structures differs significantly from those described for model A because the food web B does not provide mutual protection for a neutral pair against another

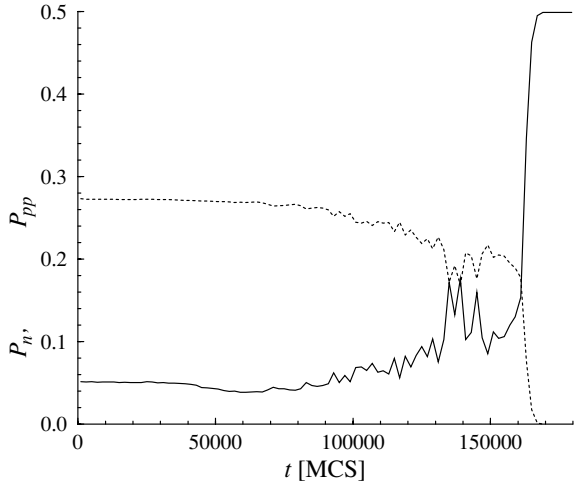

Figure 6. Time dependence of the probability of neutral (dashed line) and predator–prey (solid line) pairs for $X_s = 0.0654$ and $L = 2000$. The MC data are smoothed out by averaging over 2000 MCS.

neutral pair. Instead, the well-mixed phases of the neutral pairs destroy each other cyclically ($\Phi_{03}^{(n)}$ destroys $\Phi_{14}^{(n)}$ destroys $\Phi_{25}^{(n)}$ destroys $\Phi_{03}^{(n)}$) via a complicated process. For example, the offspring of a single species 0 can occupy the whole territory of the phase $\Phi_{14}^{(c)}$. As a result, if the growing domains of the phases $\Phi_{03}^{(c)}$ and $\Phi_{14}^{(c)}$ meet along a common boundary, then the domain $\Phi_{14}^{(c)}$ is transformed (via the invasion) into a domain of $\Phi_{0}^{(h)}$ that is also unstable against the invasions of species 2 and 5.

Within the second region of X_s the six species can coexist for a sufficiently long time in such a structure where the species with even labels are in a minority. The formation of the mixed phases of the neutral species begins in those patches where two species of minorities are missing due to the fluctuations. According to the previous analysis of the four-species subsystem b, the spontaneous formation of the well-mixed phase of the corresponding neutral species is permitted because the condition $X_s > X_{\rm cr}^{(4b)}$ is fulfilled within the given region of X_s. By this means sufficiently large domains of the states $\Phi_{03}^{(n)}$, $\Phi_{14}^{(n)}$ and $\Phi_{25}^{(n)}$ happen to form by chance. During their expansion these domains meet one of their rivals and then one of them is destroyed as described above.

Figure 6 shows the variation of $P_n(t)$ and $P_{\rm pp}(t)$ for a given X_s close to the second transition point. At the beginning these curves are smooth. Later, however, one can observe larger and larger variations reflecting the destruction of domains of types $\Phi_{03}^{(n)}$, $\Phi_{14}^{(n)}$ and $\Phi_{25}^{(n)}$ whose average size increases monotonically. The series of these larger and larger invasion processes is ended when only one of these phases prevails over the whole system.

It is conjectured that this (rock–scissors–paper like) cyclic dominance between the two-species associations plays a crucial role in the maintenance of the six-species phase.

6. Model *C*

This model has eight equivalent three-species cyclic associations as mentioned above. The simulations for a system size of $L = 400$ have justified that any of them can be the final stationary state independently of the value of X_s.

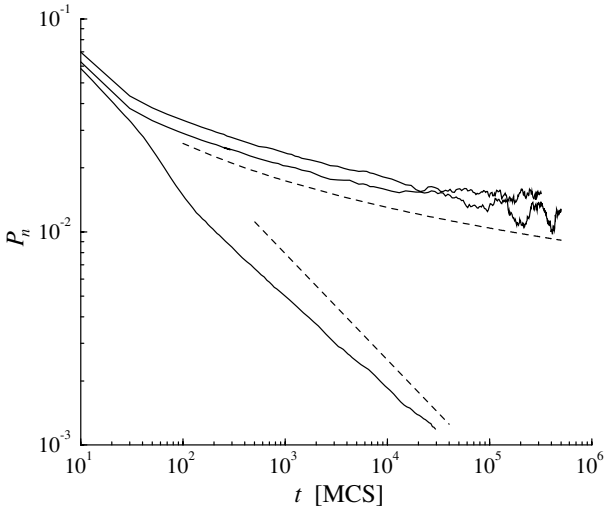

Figure 7. Log–log plot of the probability of neutral pairs versus time for $X_s = 0.05$ (upper solid line) and $X_s = 0$ (central solid line). The lower solid line shows the same quantity in the model A for $X_s = 0$. To compare the MC results with the theoretical expectations, the upper dashed line represents the function $P_n(t) = 0.12/\ln(t)$ while the lower one shows an algebraic decay, $P_n(t) = 0.25/\sqrt{t}$.

It is expected that this 'mono-domain' state is developed via a domain growing process. This phenomenon can be described by the variation of the probability of neutral pairs vanishing in the bulk of 'mono-domain' states. The results of MC simulations (for $L = 2500$) are plotted in figure 7 where the data are averaged over a sampling time increased from 2 to 2000 MCS.

Figure 7 shows that the very slow domain growing process for $X_s = 0$ becomes even slower for $X_s = 0.05$. Indeed we cannot exclude the blocking of the coarsening process as it happens in the voter model for higher dimensions ($d > 2$) [32]. Keeping in mind the large statistical uncertainties (for large times), these data recall to us the growing processes observed for the two-dimensional voter model where the concentration of domain walls vanishes as $1/\ln(t)$ plotted also in figure 7 [33, 32]. The voter model exemplifies the coarsening process in a broad class of models undergoing a phase ordering without surface tension [34]. In the present model the definition of the boundary separating two cyclic three-species phases is confusing because these phases may involve one or two common species (compare $\Phi^{(c)}_{015}$ with $\Phi^{(c)}_{012}$ or $\Phi^{(c)}_{123}$).

A strikingly different growth process is found for model A (discussed previously) where the system has only two cyclic three-species phases composed from disjoint sets of species ($\Phi^{(c)}_{024}$ or $\Phi^{(c)}_{135}$). In order to visualize the relevant differences figure 7 also shows the MC results obtained in the model A for $X_s = 0$ and $L = 4000$. These numerical results indicate that here the asymptotic behaviour of $P_n(t)$ is close to the theoretical prediction ($P_n(t) \sim 1/\sqrt{t}$) characterizing the growth controlled by the reduction of an interfacial energy [25, 27].

Evidently, further research is required to clarify those ingredients of these models that are responsible for the different growth processes. Furthermore, here it is worth mentioning that the logarithmic growth supports the maintenance of biodiversity for a very long time if the system is sufficiently large.

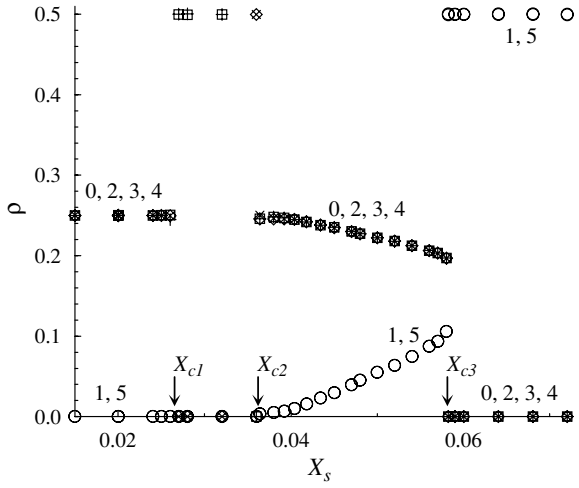

Figure 8. Concentration of species versus X_s in the model D. The MC data are denoted by symbols with fourfold symmetry (pluses, crosses, open squares and diamonds) for those species belonging to the four-species cyclic defensive alliance, and by open circles for the species 1 and 5. The arrows indicate the critical values of X_s where transitions appear.

7. Model *D*

For this food web the system has a four-species cyclic defensive alliance ($\Phi^{(c)}_{0234}$ as shown in figure 1) that is stable if $X_s = 0$ [19]. According to the simulations for weak rate of site exchange, the species 1 and 5 die out within a short transient time. In the corresponding four-species subsystem (see section 3) the cyclic invasions can sustain their coexistence if $X_s < X^{(4a)}_{\rm cr}$. For higher X_s the spatial distribution of these four species decomposes into two types of two-species domains ($\Phi^{(n)}_{03}$ and $\Phi^{(n)}_{24}$) as described above. If X_s is increased then this process becomes faster, and above a threshold value the domains of phases $\Phi^{(n)}_{03}$ and $\Phi^{(n)}_{24}$ are built up by these processes before their mortal enemies (species 1 and 5) die out. One can easily check that the species 1 (5) can occupy the whole territory of the phases $\Phi^{(n)}_{03}$ $\left(\Phi^{(n)}_{24}\right)$. Thus, for a sufficiently intensive mixing, the species 1 and 5 will have an enhanced chance to survive because they are fed by the emerging domains of $\Phi^{(n)}_{03}$ and $\Phi^{(n)}_{24}$. For large X_s this mechanism can be so effective that finally the phase $\Phi^{(n)}_{15}$ will dominate the whole system as shown in figure 8. Note that the well-mixed phase $\Phi^{(n)}_{15}$ is also a defensive alliance because species 1 and 5 protect each other against the different invaders.

Figure 8 shows that four types of final stationary states can be distinguished when X_s is increased. In the first region $\left(X_s < X^{(6D)}_{c1} = X^{(4a)}_{\rm cr}\right)$ the species of the phase $\Phi^{(c)}_{0234}$ take place with the same concentration meanwhile P_n and $P_{\rm pp}$ vary with X_s as plotted in figure 3. Starting from a random initial state, this system evolves into one of the neutral-pair phases $\Phi^{(n)}_{03}$ and $\Phi^{(n)}_{24}$ if $X^{(6D)}_{c1} < X_s < X^{(6D)}_{c2}$ where the value of $X^{(6D)}_{c2}$ depends on the size L as will be discussed below. Within the third region $\left(X^{(6D)}_{c2} < X_s < X^{(6D)}_{c3}\right)$, the six species coexist in such a way that $\rho_0 = \rho_2 = \rho_3 = \rho_4 > \rho_1 = \rho_5 > 0$. If $X_s > X^{(6D)}_{c3} = 0.0581(1)$ then only the species 1 and 5 will survive, forming a phase $\Phi^{(n)}_{15}$.

In this model the first and the third transitions exhibit a sudden change both in concentrations and in pair probabilities (P_n and $P_{\rm pp}$). However, the classification of the second transition (as well as the numerical value of $X^{(6D)}_{c2}$) is difficult because of its unusual features.

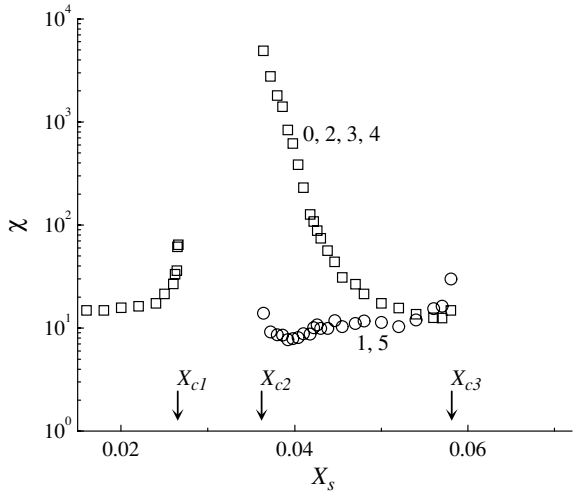

Figure 9. Fluctuation of concentration as a function of X_s for the species as denoted by the figures.

Namely, ρ_1 and ρ_5 decrease monotonically when X_s is decreased within the third region. At the same time we have observed a dramatic increase in the fluctuation of concentration for the majority species (see figure 9), meanwhile the corresponding average concentrations are close to $1/4$ (see figure 8). To avoid the undesired effects of these fluctuations the simulations were performed for such large system sizes (the linear size is increased up to $L = 2600$) where the current values of concentrations were significantly larger than the amplitude of fluctuation characterized by their standard deviation dependent on size ($\sqrt{\chi/N}$). For smaller sizes the system evolves into the phase $\Phi_{03}^{(n)}$ or $\Phi_{24}^{(n)}$.

Figure 9 demonstrates clearly the absence of fluctuations for the missing species as well as for the phases composed of neutral species. The MC data refer to an exponential increase in χ_0, χ_2, χ_3 and χ_4 if X_s approaches X_{c2} from above.

Within the region of large fluctuations the time dependence of concentrations shows the occurrence and destruction of domains with structures $\Phi_{03}^{(n)}$ and $\Phi_{24}^{(n)}$. These domains are invaded by the sparsely dispersed species 1 and 5. The resultant phase, however, is not stable at the given X_s and sooner or later the phases $\Phi_{03}^{(n)}$ or $\Phi_{24}^{(n)}$ are formed again. In some sense the evolution of the spatio-temporal pattern is similar to those described by the mentioned spatial rock–scissors–paper games [11, 13, 17] as well as in the forest-fire models [35–37]. In the present case two cycles interfere in a complex way because cyclic dominance emerges between the different sets of associations and this mechanism supports the maintenance of biodiversity with more associations (and species).

Due to the mentioned difficulties we could not determine accurately how concentrations ρ_1 and ρ_5 vanish when approaching $X_{c2}^{(6D)}$ from above. In the light of the MC results one can conclude a weakly first-order phase transition (sudden jump in $\rho_1 = \rho_5$) accompanied with an increase in $\chi_1 = \chi_5$ as illustrated in figure 9.

8. Conclusions

The numerical analysis of the four different six-species, spatial predator–prey models has highlighted the large variety of states and phenomena (transitions) that can occur in

self-sustaining, multi-species ecological systems. Due to their simplicity the present models have allowed us to consider quantitatively some interesting phenomena. Instead of recalling the curious features found for these oversimplified models, henceforth, I wish to concentrate on those general messages concluded from these examples.

One of the relevant messages is related to the increase in the degree of freedom. Many recent works are focused on spatial systems with one, two or three species. For larger number of species the present models exemplify how the simple dynamical rules build up more complex objects (alliances) that can be considered as additional species participating in the evolutionary competition. In short, the degree of freedom (here the number of species) is increased by the spontaneously occurring alliances having particular composition and spatial structure. One can believe that the food web of these systems should be extended by these complex objects (with suitable invasion rates) to have a better picture of the whole spatial system.

In the context of game theory (for details, see [1–4, 6]), the interaction of species is described by the payoff matrix (the adjacency matrix of the food web in the present models) that determines the Nash equilibrium from which the unilateral deviation yields loss. For many evolutionary (dynamical) rules the Nash equilibrium represents an evolutionary stable state under the mean-field conditions. The Nash equilibrium is not necessarily unique and it can be a mixed state (strategy). In the spatial models with short-range interactions several species can be absent from a given territory and the Nash equilibrium for the corresponding subsystem can be distinct from those characterizing the complete system. Noises affects the stability of these spatial states [38] and modifies the average velocity of invasions along the interfaces separating the competing phases [21]. The above results justify that the invasion processes between the 'stable' states of subsystems can play a crucial role in the formation of the final stationary states.

For many cases the final stationary state is reached through a coarsening process where the alliances (degenerated Nash equilibria) form growing domains. The corresponding domain growth process is affected by the additional phases (and mechanisms) along interfaces. It is not yet known how these effects modify the growth process yielding significantly slower (logarithmical) domain growth.

Most of the (first-order) transitions occur at such a value of X_s where the invasion rate between two dominant alliances vanishes as detailed previously [21]. Remarkable exceptions are the fourth transition in model B and the second one in model D. In both cases more than one species die out simultaneously and their extinction is accompanied by an enhanced concentration fluctuation for the surviving species and the resultant spatio-temporal structures can mediate unusual interactions between the vanishing species. These transitions are inherently distinct and their classification requires further time-consuming numerical investigations.

The spontaneous formation of complex spatio-temporal structures is one of the most interesting predictions of these simple models because it sustains an abundance of species. Furthermore, this feature mixes the concept of the part and whole. At the same time the corresponding system can be interpreted as a set of objects that create objects in a way characterizing living systems [39]. In the light of the present results one can easily imagine that the choice of more complex food webs can result in the emergence of more and more complex objects (e.g., alliances of alliances with particular spatio-temporal structures). Besides, these models imply the possibility that the evolution of the food web by mutations [40–42] and the evolution of the spatial ecological system are strongly related to each other while the spatial inhomogeneity can be enhanced in the system.

Acknowledgments

Supports from the Hungarian National Research Fund (T-47003) and the European Science Foundation (COST P10) are acknowledged.

References

[1] Maynard Smith J 1982 *Evolution and the Theory of Games* (Cambridge: Cambridge University Press)
[2] Weibull J W 1995 *Evolutionary Game Theory* (Cambridge, MA: MIT Press)
[3] Hofbauer J and Sigmund K 1998 *Evolutionary Games and Population Dynamics* (Cambridge: Cambridge University Press)
[4] Gintis H 2000 *Game Theory Evolving* (Princeton, NJ: Princeton University Press)
[5] Drossel B 2001 *Adv. Phys.* **50** 209
[6] Miekisz J 2004 *J. Phys. A: Math. Gen.* **37** 9891
[7] Pekalski A 2004 *Comput. Sci. Eng.* **6** 62
[8] He M F, Pan Q H and Wang S 2005 *Int. J. Mod. Phys.* C **16** 177
[9] Watt A S 1947 *J. Ecol.* **35** 1
[10] Rasmussen S *et al* 2004 *Science* **303** 963
[11] Tainaka K 1989 *Phys. Rev. Lett.* **63** 2688
[12] Sato K, Konno N and Yamaguchi T 1997 *Mem. Muroran Inst. Tech.* **47** 109
[13] Frachebourg L and Krapivsky P L 1998 *J. Phys. A: Math. Gen.* **31** L267
[14] Tainaka K 1993 *Phys. Lett.* A **176** 303
[15] Frean M and Abraham E D 2001 *Proc. R. Soc.* B **268** 1
[16] Tainaka K and Itoh Y 1991 *Europhys. Lett.* **15** 399
[17] Szabó G and Szolnoki A 2002 *Phys. Rev.* E **65** 036115
[18] Boerlijst M C and Hogeweg P 1991 *Physica* D **48** 17
[19] Szabó G and Czárán T 2001 *Phys. Rev.* E **64** 042902
[20] Sato K, Yoshida N and Konno N 2002 *Appl. Math. Comput.* **126** 255
[21] Szabó G and Sznaider G A 2004 *Phys. Rev.* E **69** 031911
[22] Ravasz M, Szabó G and Szolnoki A 2004 *Phys. Rev.* E **70** 012901
[23] Traulsen A and Schuster H G 2003 *Phys. Rev.* E **68** 046129
[24] Traulsen A and Claussen J C 2004 *Phys. Rev.* E **70** 046128
[25] Bray A J 1994 *Adv. Phys.* **43** 357
[26] Wu F Y 1982 *Rev. mod. Phys.* **54** 235
[27] Grest G S, Anderson M P and Srolovitz D J 1988 *Phys. Rev.* B **38** 4752
[28] Janssen H K 1981 *Z. Phys.* B **42** 151
[29] Grassberger P 1982 *Z. Phys.* B **47** 365
[30] Marro J and Dickman R 1999 *Nonequilibrium Phase Transitions in Lattice Models* (Cambridge: Cambridge University Press)
[31] Hinrichsen H 2000 *Adv. Phys.* **49** 815
[32] Ben-Naim E, Frachebourg L and Krapivsky P L 1996 *Phys. Rev.* E **53** 3078
[33] Liggett T M 1985 *Interacting Particle Systems* (New York: Springer)
[34] Dornic I *et al* 2001 *Phys. Rev. Lett.* **87** 045701
[35] Bak P, Chen K and Tang C 1990 *Phys. Lett.* A **147** 297
[36] Drossel B and Schwabl F 1993 *Phys. Rev. Lett.* **69** 1629
[37] Grassberger P 1993 *J. Phys. A: Math. Gen.* **26** 1081
[38] Miekisz J 2004 *J. Stat. Phys.* **117** 99
[39] Crutchfield J P and Görnerup O 2004 *Preprint* nlin.AO/0406058
[40] Drossel B, Higgs P G and McKane A J 2001 *J. Theor. Biol.* **208** 91
[41] Holt R D 2002 *Ecol. Res.* **17** 261
[42] Chowdhury D and Stauffer D 2003 *Phys. Rev.* E **68** 041901